Proceeding Paper

Performance of Fe-Rich Alkali-Activated Materials in Na_2SO_4 Solution: Role of MgO/(MgO + CaO) in the Slag [†]

Nana Wen [1,2,*] **, Arne Peys** [3] **, Tobias Hertel** [1] **and Yiannis Pontikes** [1]

1 Department of Materials Engineering, Katholieke Universiteit Leuven (KU Leuven), 3001 Leuven, Belgium; tobias.hertel@kuleuven.be (T.H.); yiannis.pontikes@kuleuven.be (Y.P.)
2 Strategic Initiative Materials (SIM vzw), Technologiepark 935, 9052 Zwijnaarde, Belgium
3 Sustainable Materials Management, Flemish Institute for Technological Research (VITO), Boeretang 200, 2400 Mol, Belgium; arne.peys@vito.be
* Correspondence: nana.wen@kuleuven.be
† Presented at International Conference on Raw Materials and Circular Economy, Athens, Greece, 5–9 September 2021.

Abstract: To enable the usage of non-ferrous metallurgy slags in alkali-activated materials (AAMs), the influence of the chemical composition of slags on durability must be better understood. In this work, two slags were synthesized with different MgO/(MgO + CaO) weight ratios to investigate the effect on the sulfate resistance (Na_2SO_4) of AAMs. Experimental results suggested that a higher MgO/(MgO + CaO) ratio does not lead to higher strength, but the trend of the mass change and compressive strength change of two AAMs is quite similar upon Na_2SO_4 exposure for 24 weeks. The leaching of elements (Na, Al, and Si) during Na_2SO_4 exposure is more significant in the early stage, while Ca leaching is more pronounced in the late stage.

Keywords: Fe-rich slag; alkali-activated material; MgO; CaO; sulfate resistance

1. Introduction

Cement has shaped much of the built environment. Due to its ubiquitous presence, cement is the source of 8% of anthropogenic CO_2 emissions [1]. Numerous efforts have been made to decrease the consumption of cement, and alkali-activated material (AAM) is one of the binder types trying to drum up greater support for sustainable alternatives. AAMs are derived from precursors (e.g., metakaolin, ferrous and non-ferrous slag, fly ash, clay, etc.) and alkali activators. Previous studies on non-ferrous slag (NFS)-based AAMs showed high reactivity and mechanical performance [2], but in order to ensure long-term performance, studies on durability are necessary. Sodium sulfate attack has been a major durability problem for cement as the sulfate ions react with the calcium and aluminate component of cement and produce ettringite and gypsum [3].

In alkali-activated blast furnace slags, slag chemistry plays an important role in chemical resistance [4]. From existing literature, Mg concentration could possibly improve the intrinsic durability of AAMs because of the layered double hydroxide phase formed [5]. There is no knowledge on this topic for alkali-activated NFSs.

Ca and Mg both take the role of network modifier cations in AAMs. In order to be able to distinguish the different roles of Ca and Mg in resisting this degradation mechanism, two NFSs were synthesized to evaluate the role of the MgO/(MgO + CaO) weight ratio in the resistance of NFS-AAM to sodium sulfate attack. During a sodium sulfate attack for 24 weeks, mass and compressive strength change were measured to evaluate the degradation.

2. Materials and Methods

Two slags were synthesized which mimicked the chemical composition of industrial slags from non-ferrous metallurgy. Melting was carried out in an induction furnace

(Indutherm TF4000) and the slags were water-quenched in order to reach a high amorphous phase [6]. The detailed production process is described elsewhere [6,7]. The quenched slags were milled using an attritor ball mill until a Blaine surface area of around 4000 ± 200 cm^2/g was reached. The chemical composition of the slags was assessed by a WD-XRF (wavelength dispersive X-ray fluorescence) spectrometer (Bruker S8).

Sodium silicate ($Na_2O \cdot 1.65\ SiO_2$, 65% H_2O) was used as the alkali activator. Sodium hydroxide pellets were dissolved in commercial sodium silicate solution ($Na_2O \cdot 3.3\ SiO_2$, 63.5 wt% H_2O) and deionized water to produce the desired alkaline solution.

AAM pastes were prepared by mixing the slag and activator at a mass ratio of 0.4 with a hand mixer for 3 min. Sample dimensions were $20 \times 20 \times 20$ mm^3 and triplicates were prepared. Cubic samples were kept in an air-tight plastic box in an air-conditioned room (20 ± 2 °C; 50 ± 5% relative humidity) for 28 days before immersion in 5 wt% Na_2SO_4 solution for 24 weeks using a sulfate solution to paste mass ratio of 8. The Na_2SO_4 solution was renewed every 4 weeks. The degradation of the specimens was evaluated by the change in mass and compressive strength. At the aimed date, samples were taken out from the Na_2SO_4 solution, dried with paper, and the mass or compressive strength was recorded (triplicates for each formulation). The compressive strength was tested using an Instron 5985 testing device at a displacement rate of 2 mm/min.

The concentration of Na, Ca, Al, and Si in the pregnant Na_2SO_4 solution and the pH of this solution were detected using ICP-OES (Varian-720 ES) and a pH meter (Metter Toledo), respectively. Additionally, the before and after exposure of AAM to the sulfate solution was studied by attenuated total reflectance–Fourier transform infrared (ATR–FTIR) spectroscopy (Bruker Alpha-P).

3. Results and Discussion

The chemical composition of the two slags is shown in Table 1. To study the role of the MgO/(MgO + CaO) weight ratio, M0 and M0.4 have similar chemical compositions with the exception that for M0.4 4wt% CaO was replaced by MgO compared to M0. The weight ratios between all other elements are relatively constant.

Table 1. Chemical composition of slags (wt%), obtained by XRF.

	FeO	SiO$_2$	CaO	Al$_2$O$_3$	MgO	MgO/(MgO + CaO)
M0	48.0	34.0	10.5	7.5	0	0
M0.4	49.0	33.0	6.5	7.5	4.0	0.4

Figure 1a depicts the mass change for AAM samples in sodium sulfate solution for 24 weeks. Both samples recorded a decrease in mass throughout the exposure. The mass losses for the AAMs produced from M0 and M0.4 are similar.

The compressive strength evolution over time for AAMs exposed to sodium sulfate is presented in Figure 1b. Strength at time 0 means the unexposed samples at 28 days. The strength of the M0 samples is, thus, slightly higher than that of the M0.4 samples—58 MPa instead of 49 MPa. For both samples, the increase in compressive strength was measured; the compressive strength for M0–AAM stayed higher than that of M0.4–AAM at all testing dates. The increase in the strength of AAMs exposed to the sulfate solution indicates the slag probably dissolved more and the Fe-rich slag-based AAMs are resistant to Na_2SO_4 attack. This is in agreement with the results in alkali-activated blast furnace slags [8], where they found that the chemistry and structure of AAMs is essentially immune to Na_2SO_4 solution.
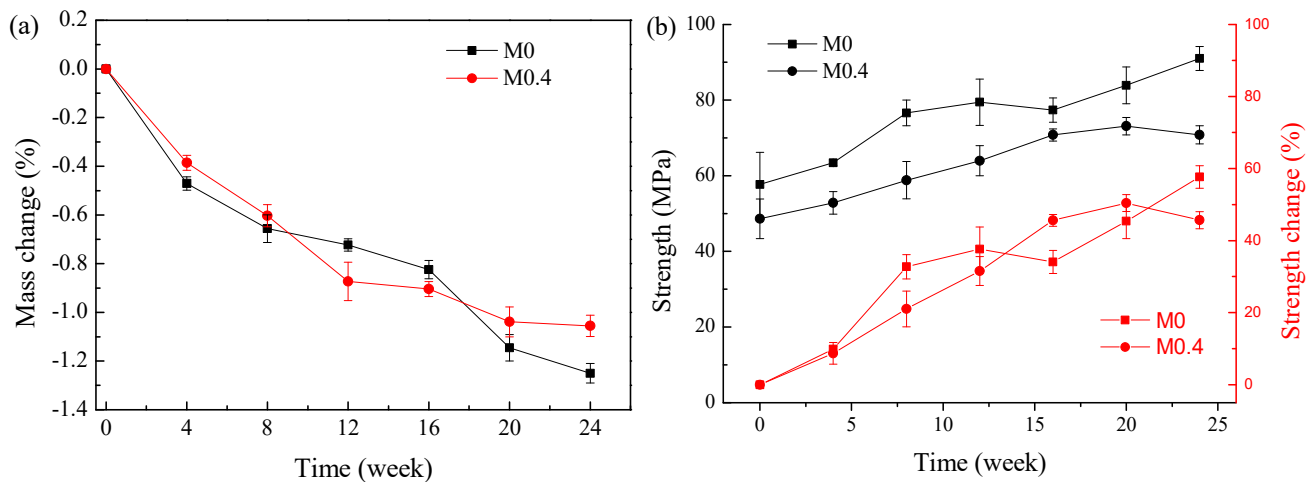
Figure 1. Mass and compressive strength changes at various times for AAMs in sodium sulfate solution. (**a**) Mass change; (**b**) compressive strength and compressive strength change.

The pregnant sulfate solution was analyzed using ICP-OES and the concentrations of Na, Ca, Al, and Si in the solution are summarized in Table 2. Fe and Mg cannot be detected as Fe and Mg precipitate in high basic solutions. Na, Al, and Si leached more significant from the beginning, and gradually leached less over the exposure time. The leaching behavior of Ca was different. The concentration of Ca gradually increased and the highest concentration was recorded in the last cycle from week 20 to week 24. The initial weight ratio in CaO between M0.4 and M0 was 0.62 (6.5/10.5). The Ca weight ratio in the pregnant solution ranged from 0.262 to 0.506 and increased with time. Even relative to the chemical composition, more Ca leached out from M0 during the 24-week exposure to the Na_2SO_4 solution. More Al and Si leached from the M0–AAM in the first 8 weeks, and later on, the concentrations in the leachate from the M0.4–AAM were slightly higher.

Table 2. Elements concentration of AAMs in sodium sulfate solution for certain ages (ppm) (deviation inside the bracket).

	M0-AAM				M0.4-AAM			
	Na	**Ca**	**Al**	**Si**	**Na**	**Ca**	**Al**	**Si**
Week 2	673 (52)	4.0 (0.13)	2.7 (0.14)	21.0 (1)	747 (63)	1.3 (0.3)	1.6 (0.02)	17.2 (0.1)
Week 4	1275 (10)	5.3 (0.8)	3.1 (0.1)	26.8 (0.1)	1047 (77)	1.4 (0.3)	1.9 (0.02)	22.4 (0.1)
Week 8	623 (66)	13.2 (0.3)	1.0 (0.01)	8.4 (0.2)	503 (71)	5.5 (0.3)	1.1 (0.07)	12.1 (0.2)
Week 16	410 (60)	25.1 (0.7)	0.4 (0.03)	3.0 (0.2)	487 (61)	12.7 (0.2)	0.5 (0.02)	5.3 (0.2)
Week 24	340 (55)	33.2 (0.7)	0.4 (0.01)	3.3 (0.1)	463 (59)	16 (0.2)	0.4 (0.01)	4.2 (0.2)

The pH results of the used solution are presented in Figure 2. The starting pH of the 5 wt% Na_2SO_4 solution was 8.23. After AAM samples were immersed into the sulfate solution, the pH increased. The increase in pH value can be attributed to the diffusion of OH^- ions from the pore solution of the matrix into the sulfate solution [3]. Since the sulfate solution was completely replaced every cycle (1 cycle = 4 weeks), the increase in pH with respect to the starting pH of the Na_2SO_4 solution for each cycle decreased. From Figure 2, it can also be seen that the pH of the two AAMs is quite similar.
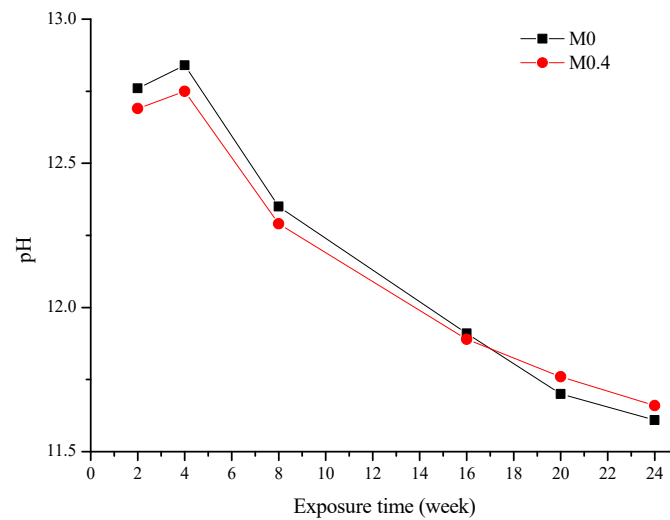
Figure 2. pH of the used solution at various ages.

Since XRD patterns of the slags and AAMs before and after exposure did not show any crystalline phases (not shown for the sake of brevity), FTIR was chosen to investigate the influence of MgO/(MgO + CaO) on sulfate resistance. Figure 3a illustrates the FTIR spectra of AAMs unexposed and exposed to sulfate solution. There are no clear changes, such as new or disappearing bands, when comparing AAMs before and after exposure to the sulfate solution, which indicates that the silicate network is not significantly altered. A zoomed-in spectrum focused on the Si–O stretching band (1200–700 cm^{-1}), Figure 3b, enables a more detailed analysis. After exposure, the maximum of the main band slightly shifted to a lower wavenumber and the extent of the shifting is more obvious for M0.4 (from 986 to 974 cm^{-1}) than M0 (from 978 to 976 cm^{-1}). The main change in both AAMs is broadening of the band, seemingly caused by the appearance of a shoulder at the two sides of the band. The signals are broad and, thus, confirm that the presence of crystalline precipitates is unlikely. The high wavenumber shoulder around 1100 cm^{-1} indicates the presence of sulfates [9]. The low wavenumber shoulder (850–900 cm^{-1}) cannot be explained by the presence of sulfates. Other possible explanations are (1) the incorporation of additional Na in the silicate network; therefore, increase in network modifying cations or (2) a more drastic reconfiguration of the binding phases due to the change in pH of the pore solution.
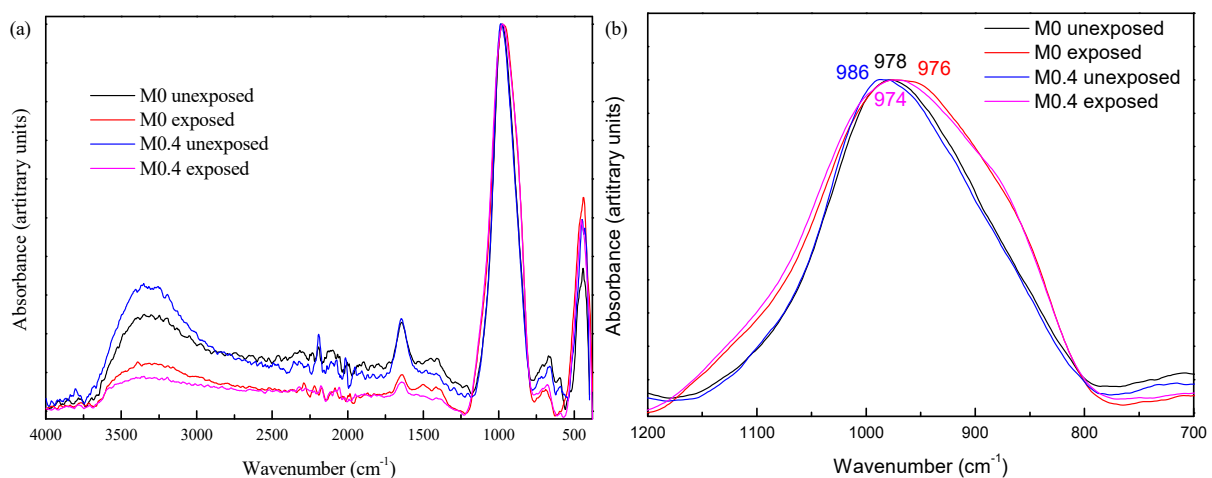

Figure 3. The FTIR spectra of AAM before and after exposure to sodium sulfate solution. (**a**) Full spectra; (**b**) zoom on the Si–O stretching band.

4. Conclusions

Experimental findings of the M0–AAM and M0.4–AAM exposure to sodium sulfate solution for 24 weeks indicated that non-ferrous metallurgy slags with different MgO/(MgO + CaO) weight ratios result in AAMs with high sulfate resistance. A similar mass change and compressive strength patterns were observed despite the different starting strength 28 days after mixing. Leaching during Na_2SO_4 exposure for low MgO/(MgO + CaO) is more significant in the early stage but slightly less than high MgO/(MgO + CaO) in the late stage. FTIR results indicated that sulfate attack does not have a significant impact on the structure of both Fe-rich AAMs.

Author Contributions: Conceptualization, N.W., A.P. and T.H.; methodology, N.W.; software, N.W.; validation, N.W., A.P., T.H. and Y.P.; formal analysis, N.W., A.P. and T.H.; investigation, N.W.; resources, N.W.; data curation, N.W.; writing—original draft preparation, N.W.; writing—review and editing, A.P., T.H. and Y.P.; visualization, N.W.; supervision, A.P., T.H. and Y.P.; project administration, Y.P. All authors have read and agreed to the published version of the manuscript.

Institutional Review Board Statement: Not applicable.

Informed Consent Statement: Not applicable.

Data Availability Statement: The data presented in the study are available on request from the corresponding author.

Conflicts of Interest: The authors declare no conflict of interest.

References

1. Habert, G.; Miller, S.A.; John, V.M.; Provis, J.L.; Horvath, A.; Horvath, A.; Scrivener, K.L. Environmental impacts and decarbonization strategies in the cement and concrete industries. *Nat. Rev. Earth Environ.* **2020**, *1*, 559–573. [CrossRef]
2. Onisei, S.; Lesage, K.; Blanpain, B.; Pontikes, Y. Early Age Microstructural Transformations of an Inorganic Polymer Made of Fayalite Slag. *J. Am. Ceram. Soc.* **2015**, *98*, 2269–2277. [CrossRef]
3. Komljenović, M.; Baščarević, Z.; Marjanović, N.; Nikolić, V. External sulfate attack on alkali-activated slag. *Constr. Build. Mater.* **2013**, *49*, 31–39. [CrossRef]
4. Bernal, S.A.; Provis, J.L. Durability of Alkali-Activated Materials: Progress and Perspectives. *J. Am. Ceram. Soc.* **2014**, *97*, 997–1008. [CrossRef]
5. Ke, X.; Bernal, S.A.; Provis, J.L. Uptake of chloride and carbonate by Mg-Al and Ca-Al layered double hydroxides in simulated pore solutions of alkali-activated slag cement. *Cem. Concr. Res.* **2017**, *100*, 1–13. [CrossRef]
6. Siakati, C.; Douvalis, A.P.; Ziogas, P.; Peys, A.; Pontikes, Y. Impact of the solidification path of $FeOx$–SiO_2 slags on the resultant inorganic polymers. *J. Am. Ceram. Soc.* **2019**, *103*, 2173–2184. [CrossRef]
7. Wen, N.; Peys, A.; Hertel, T.; Pontikes, Y. The effect of the chemical composition of MgO-CaO-FeO-Al_2O_3-SiO_2 slag on the reaction kinetics and compressive strength of alkali-activated materials. In Proceedings of the 7th International Slag Valorisation Symposium, Leuven, Belgium, 27–29 April 2021; pp. 270–275.
8. Gong, K.; White, C.E. Nanoscale Chemical Degradation Mechanisms of Sulfate Attack in Alkali-activated Slag. *J. Phys. Chem. C* **2018**, *122*, 5992–6004. [CrossRef]
9. Takahashi, T.; Maehara, I.; Kaneko, N. Infrared reflection spectra of gypsum. *Spectrochim.* **1983**, *39*, 449–455. [CrossRef]